AIP | APL Materials

Probing orbital ordering in LaVO3 epitaxial films by Raman scattering

I. Vrejoiu, C. Himcinschi, L. Jin, C.-L. Jia, N. Raab, J. Engelmayer, R. Waser, R. Dittmann, and P. H. M. van Loosdrecht

Citation: APL Mater. **4**, 046103 (2016); doi: 10.1063/1.4945658
View online: http://dx.doi.org/10.1063/1.4945658
View Table of Contents: http://scitation.aip.org/content/aip/journal/aplmater/4/4?ver=pdfcov
Published by the AIP Publishing

APL MATERIALS **4**, 046103 (2016)

Probing orbital ordering in $LaVO_3$ epitaxial films by Raman scattering

I. Vrejoiu,[1,a] C. Himcinschi,[2,a] L. Jin,[3] C.-L. Jia,[3] N. Raab,[4] J. Engelmayer,[1] R. Waser,[4] R. Dittmann,[4] and P. H. M. van Loosdrecht[1]
[1]*Physikalisches Institut, University of Cologne, D-50937 Cologne, Germany*
[2]*TU Bergakademie Freiberg, Institute of Theoretical Physics, D-09596 Freiberg, Germany*
[3]*Peter Grünberg Institut (PGI-5), Forschungszentrum Jülich GmbH, D-52425 Jülich, Germany*
[4]*Peter Grünberg Institut (PGI-7), Forschungszentrum Jülich GmbH, D-52425 Jülich, Germany*

(Received 16 February 2016; accepted 22 March 2016; published online 8 April 2016)

Single crystals of Mott-Hubbard insulator $LaVO_3$ exhibit spin and orbital ordering along with a structural change below ≈140 K. The occurrence of orbital ordering in epitaxial $LaVO_3$ films has, however, been little investigated. By temperature-dependent Raman scattering spectroscopy, we probed and evidenced the transition to orbital ordering in epitaxial $LaVO_3$ film samples fabricated by pulsed-laser deposition. This opens up the possibility to explore the influence of different epitaxial strain (compressive *vs*. tensile) and of epitaxy-induced distortions of oxygen octahedra on the orbital ordering, in epitaxial perovskite vanadate films.
[http://dx.doi.org/10.1063/1.4945658]

Transition-metal oxides, for which strong electron correlations play an important role, exhibit a wide spectrum of intriguing physical properties, such as Mott transitions, colossal magnetoresistance, and high T_C-superconductivity. $LaVO_3$ is a prototypical Mott-Hubbard insulator with a $3d^2$ electronic configuration of V^{3+}. At 143 K, $LaVO_3$ single crystals undergo a magnetic transition from a paramagnetic state to an antiferromagnetic state and a first order structural phase transition from orthorhombic *Pbnm* to monoclinic $P2_1/b$ following right below the magnetic ordering temperature, at 141 K.[1,2] The antiferromagnetic state is a C-type spin-ordered (C-type SO) state with ferromagnetically arranged $V^{3+}(S = 1)$ spins along the *c*-axis and the antiferromagnetic alignment in the *ab* plane. Along with the structural transition, a G-type orbital order (G-type OO) sets in below 141 K as well, with commonly occupied t_{2g} d_{xy} orbitals and d_{yz} or d_{zx} orbitals that are alternately occupied in all directions.

Concerning the motivation for thin films of Mott insulators, an exciting application is their use as the active material in resistive random access memories.[3] Particular interest in epitaxial $LaVO_3$ films has been driven by the "polar discontinuity" at the interface $LaVO_3/SrTiO_3$, analogues to the $LaAlO_3/SrTiO_3$ case.[4,5] The fabrication of phase pure $LaVO_3$ films, however, requires oxygen pressures lower than about 10^{-5} mbar, so that the competing $LaVO_4$ phase does not form. The fabrication of the $LaVO_x$ films under high vacuum conditions affects the stoichiometry of the film and oxygen content of the $SrTiO_3$ substrates. The surface of $SrTiO_3$ substrates may become reduced,[6] and this affects the transport properties of the $LaVO_x/SrTiO_3$ samples dramatically.[7] Temperature-dependent transport properties of $LaVO_x$ films grown on $SrTiO_3$, showing either metallic[4,8] or an overlapping two-component metallic and semiconducting behavior,[7–9] are influenced by contributions from the oxygen-deficient substrate. Similar issues have been encountered

[a]Authors to whom correspondence should be addressed. Electronic mail: vrejoiu@ph2.uni-koeln.de and himcinsc@physik.tu-freiberg.de.

for the assessment of the properties of epitaxial $LaTiO_3$ thin films, whose growth also requires high vacuum conditions.[10] The role played in epitaxial film properties by $SrTiO_3$ substrates, which are prone to change readily the oxygen content and the transport properties under reducing conditions, was brought into focus, e.g., by Schneider *et al.*[11]

In contrast, the transport properties of $LaVO_x$ films grown on $DyScO_3(110)$ (DSO) substrates, under the same conditions as films grown on $SrTiO_3$ (100) (STO), indicate semiconducting behavior of the vanadate films.[8] The resistance of the $LaVO_x$ films on DSO substrates increased with decreasing temperature and only the resistivity data down to about 180 K were shown by He *et al.*[8] Although the transport properties of the $LaVO_3$ films grown on DSO exhibit the semiconducting behavior expected for a Mott insulating material, $DyScO_3$ crystals are paramagnetic[12] and hinder strongly the magnetic measurements of $LaVO_3$ films. Temperature-dependent magnetic susceptibility and magnetization measurements of $LaVO_3$ single crystals yielded direct information about the antiferromagnetic order and the corresponding transition temperatures.[13,14] However, so far no systematic measurements have been published for $LaVO_3$ epitaxial films. There exists a report on the magnetic properties of $PrVO_3$ epitaxial films grown on STO(100), for which a surprisingly reduced SO temperature of 80 K (in bulk, the antiferromagnetic SO temperature is 140 K) and a hard-ferromagnetic behavior at 10 K were observed.[15]

Probably due to these experimental difficulties, so far the ordering phenomena in epitaxial perovskite vanadate film samples have not been properly addressed. Optical spectroscopy investigations provide alternative methods for studying orbital ordering transitions in $LaVO_3$ films. Though also these techniques may suffer from hindering contributions from the substrates, they are potentially easier methods to separate the substrate and film contributions by making use of the specific spectral film/substrate features. Temperature-dependent Raman scattering and optical conductivity investigations of $LaVO_3$ single crystals were performed in great detail, in order to study the coupling between structure and electronic properties in the SO and OO states.[2,16–20]

Here we investigate the structural phase transitions and the onset of the orbital ordering in $LaVO_3$ epitaxial films fabricated by pulsed-laser deposition (PLD). Temperature-dependent Raman scattering spectroscopy was employed to monitor the occurrence of orbital ordering and its associated structural phase transition in $LaVO_3$ epitaxial films. To the best of our knowledge, neither Raman spectroscopy studies nor experimental evidence of orbital ordering occurring in $LaVO_3$ film samples has been reported so far.

Epitaxial growth of $LaVO_3$ films has been achieved by a variety of techniques, predominantly by PLD[4,5,7–9,21] or by molecular beam epitaxy.[22] The stabilization of the perovskite $LaVO_3$ phase in thin films was successful by performing the growth in either high vacuum[4,5,7–9,22] or in pure Ar or Ar/H_2 atmosphere.[9,21] We fabricated the films by PLD using a KrF excimer laser. The chamber was evacuated down to less than 10^{-7} mbar. STO(100), DSO(110), and twinned $LaGaO_3(110)/(001)$ (LGO) single crystal substrates were employed. The substrates were heated to temperatures of about 450 °C in high vacuum conditions. Then Ar/4% H_2 gas mixture was let in the PLD chamber to pressures of $\approx 10^{-3}$ mbar and the substrates were further heated to 700 °C and the films were grown under these conditions. In the same PLD system, using moderate pressures of 4×10^{-4} mbar, Ar/H_2 was successful for the growth of films of other materials that require reducing conditions, such as $EuTiO_3$ films.[23]

A laser fluence of 1.2 J/cm^2 was employed for the ablation of the $LaVO_4$ ceramic target and the laser repetition rate was 3 Hz. After growth, the samples were cooled to room temperature (RT) in the same Ar/H_2 atmosphere. Reflective high energy electron diffraction (RHEED) was used to monitor the growth and estimate the growth rate of the $LaVO_3$ films.

Raman scattering spectra were recorded in back-scattering configuration using a Horiba-Jobin-Yvon Labram HR 800 spectrometer equipped with an Olympus Microscope, a 600 grooves/mm grating, and a Peltier cooled CCD detector. For excitation, the 632.8 nm (1.96 eV) line of a HeNe laser was used. The beam was focused on the sample (spot size of ≈ 2.5 μm) and collected through a 50× magnification long distance microscope objective (numerical aperture NA = 0.55). To avoid sample heating, the laser power at the sample was kept below 1.5 mW. Temperature-dependent Raman measurements from 87 K up to room temperature were carried out with a Linkam THMS-600 cooling-heating stage placed under the Raman microscope. For each temperature, two

measurements were done: for the first measurement, the laser was focused at the sample surface (film/substrate signal); during the second, the laser was focused about 20 μm under the sample surface (substrate signal).[24] The Raman scattering signal belonging to the $LaVO_3$ films was obtained by normalizing the two spectra and subsequent subtraction.

Atomic force microscopy (AFM) scans of the samples confirmed the layer-by-layer growth mode (see the topography images in Fig. 1) of the films on all substrates, which was also indicated by RHEED patterns observed during the film growth (Fig. 1, left). The layer-by-layer growth was readily achieved on all the substrates, especially if the crystals had been annealed prior to being used for PLD. The only substrates that were not annealed were the LGO crystals, in order to avoid

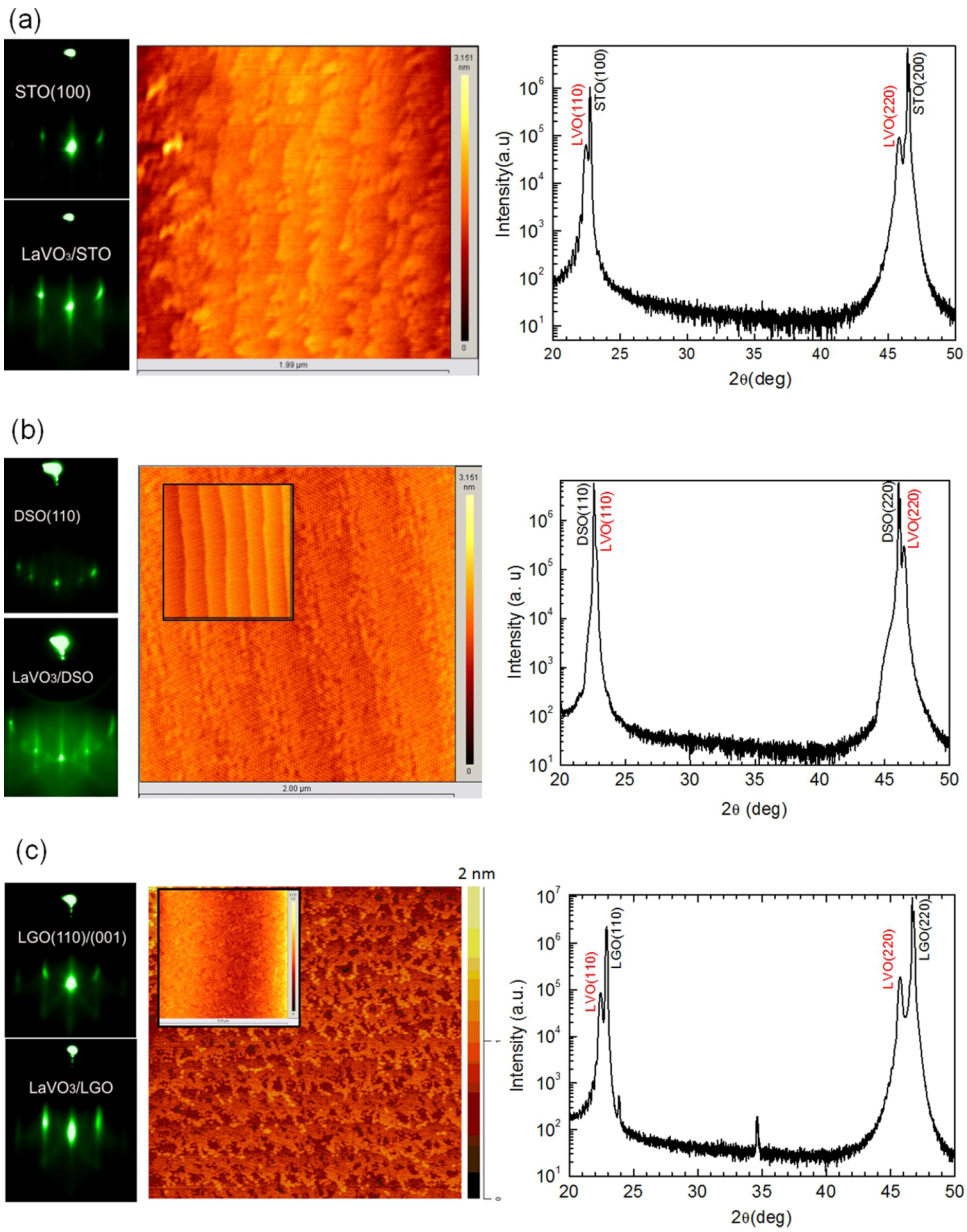

FIG. 1. Morphological and structural characterization of (a) $LaVO_3$ films grown on $SrTiO_3$(100), (b) on $DyScO_3$(110), and (c) on twinned $LaGaO_3$(110)/(001): RHEED patterns of the substrates and films (on the left), atomic force microscopy images (middle), and $2\theta-\omega$ XRD scans (right). The inset in the AFM image from panel (b) shows also the surface morphology of the annealed $DyScO_3$(110) crystal and in (c) of the as-received $LaGaO_3$(110) crystal, prior to being used for film growth. AFM images in (a) and (b) show scans over 2 μm×2 μm areas and in (c) over 5 μm×5 μm areas.

possible mechanical damage occurring during the structural phase transition at 423 K, but also in this case, layer-by-layer growth was achieved.

$LaVO_3$ crystallizes at RT in an orthorhombic structure (*Pbnm*), with lattice parameters a = 5.555 Å, b = 5.553 Å, and c = 7.849 Å and thus $a \approx b \approx c/\sqrt{2}$.[1,13,14,25–27] The low temperature phase is monoclinic $P2_1/b$, with a rather larger change of the c-axis. The structure of $LaVO_3$ exhibits tilted VO_6 octahedra and displaced La ions (with respect to a pure perovskite structure), which in case of the bulk are relatively small and the lattice parameters can be related to a pseudocubic (PC) structure according to the relation: $a_{PC,LaVO_3} \approx a/\sqrt{2} \approx b/\sqrt{2} \approx c/2$ = 3.926 Å. The lattice match of $LaVO_3$ is fairly good with the cubic STO(100) or pseudocubic LGO(110) and DSO(110) substrates ($a_{PC,LGO110}$ = 3.89 Å; a_{STO} = 3.905 Å; $a_{PC,DSO110}$ = 3.95 Å).

$2\theta - \omega$ X-ray diffraction (XRD) scans demonstrate that the $LaVO_3$ films on both substrates are epitaxial and phase pure (Fig. 1, right). For the film grown under compressive stress on STO(100), the average out-of-plane lattice parameter of our $LaVO_3$ films is about 3.955 Å and thus larger than $a_{PC,LaVO_3} \approx$ 3.926 Å. The value is in good agreement with the out-of-plane lattice parameter reported for stoichiometric $LaVO_3$ films grown on STO(100) by molecular beam epitaxy.[22] Zhang *et al.*[22] commented that, unlike in the well-studied case of epitaxial $SrTiO_3$ films,[28] for which the out-of-plane lattice parameter expands with increasing amounts of cation non-stoichiometry, the opposite trend was found for $LaVO_3$ films. For the film grown under even higher levels of compressive stress on LGO(110), the average out-of-plane lattice parameter of our $LaVO_3$ films is about 3.96 Å. On the other hand, the average out-of-plane lattice parameter for $LaVO_3$ grown on DSO(110) is about 3.905 Å, which is slightly smaller than the $a_{PC,LaVO_3} \approx$ 3.926 Å, due to the tensile epitaxial strain conditions. $2\theta - \omega$ XRD scans do not allow us to distinguish between (110)-oriented and (001) oriented growths of $LaVO_3$. It has been recently theoretically argued that there is no clear energetic preference toward one of these orientations for epitaxially strained $LaVO_3$, both under compressive and tensile strain.[27] Experimentally, so far only the structure and orientation of $PrVO_3$ and $LaVO_3$ films grown under compressive strain on $SrTiO_3$(100) have been studied, and only domains with the c-axis lying in the plane of the $SrTiO_3$ substrate were found.[15,26,29]

The orientation of the c-axis is very important for making the right choice of the polarization of the incident light in optical spectroscopy investigations.[19,20,30] To obtain more information on the epitaxial relationships between the films and the substrates and on the domain structure of the films, we performed transmission electron microscopy of cross sectional specimens. Scanning transmission electron microscopy (STEM) investigations of $LaVO_3$ films grown on cubic STO(100) crystals revealed that the films grow with the long orthorhombic c-axis of the $LaVO_3$ oriented in-plane of the substrate. Figure 2 shows a summary of the investigations of a 33 nm thick $LaVO_3$ film grown on STO(100). Two types of domains, both with the c-axis lying in the plane of the STO substrate but rotated 90° with respect to each other, were identified.[26] High angle annular dark field (HAADF)-STEM images taken in two such domains are shown in Figs. 2(b) and 2(c). The orientation of the orthorhombic unit cell in the two domains was determined by performing Fourier transform of the images, as shown in Figs. 2(d) and 2(e), where also structural models for the two domains are schematically proposed. Structural defects, most likely anti-phase boundaries, present in the $LaVO_3$ films can be better seen at higher magnification, as marked by the box in Fig. 2(f) and zoomed-in in Fig. 2(g).

Figure 3 summarizes the STEM of a 52 nm thick $LaVO_3$ film deposited on DSO. Most of the layer has a (110) orientation, i.e., the long c-axis lies in the plane of the DSO(110) substrate. However, there are also domains with the c-axis oriented perpendicular to the substrate surface. Figure 3(b) shows two neighboring domains for which the c-axis is oriented in-plane, pointing towards the viewer (on the left side of the image), and out-of-plane with respect to the DSO(110) substrate. Analysis of the Fourier transforms of the images in the two regions allowed us to determine the orientation of the orthorhombic c-axis of the $LaVO_3$. Antiphase boundaries are present at the intersection of the domains, similar to what was observed for the $LaVO_3$ grown on STO. In Fig. 3(c), an annular bright field (ABF)-STEM image taken in a domain with in-plane c-axis orientation is shown and the oxygen column position can be thus viewed, allowing the visualisation of the zigzag VO_6 tilts corresponding to the slightly distorted orthorhombic structure of the $LaVO_3$ film.[29]

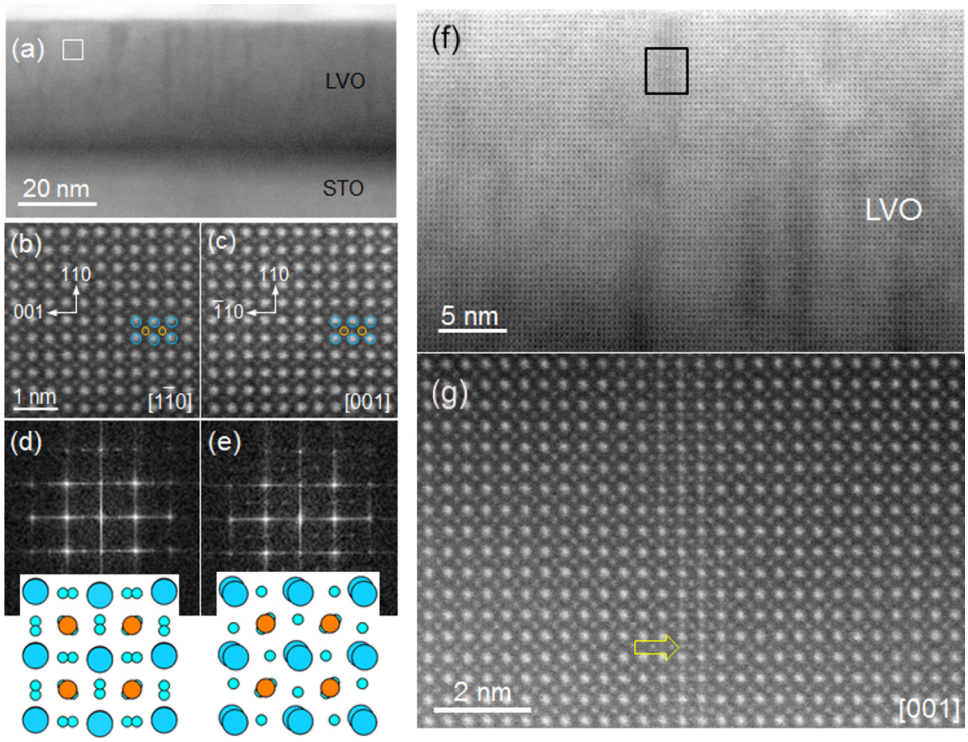

FIG. 2. Cross section HAADF-STEM investigations of a 33 nm thick $LaVO_3$ film grown on $SrTiO_3$(100): (a) low magnification overview image with a white box indicating where the high magnification images from (b) and (c) were taken; ((b) and (d)) high magnification image of a domain with the $[001]_o$ *c*-axis pointing to the left and its corresponding fast Fourier transform (FFT) with structure model below; ((c) and (e)) high magnification image of a domain with the $[001]_o$ *c*-axis pointing to the viewer and the corresponding FFT of the image with proposed structure model below; ((f) and (g)) anti-phase boundaries defects are present in the film, as marked by the black box in (g) and by the yellow arrow at higher magnification view in (f).

For the $LaVO_3$ film deposited on twinned (110)/(001)LGO substrate, we expect that both domains with the c-axis in-plane (on top of (110)LGO) and out-of-plane (on top of (001)LGO) form as well, as confirmed by the Raman data (*vide infra*).

We performed temperature-dependent in plane *dc* resistivity measurements on a 40 nm thick $LaVO_3$ film grown on DSO(110) substrate (not shown). The resistance of the $LaVO_3$ film increased rapidly with decreasing temperature, so that the measurements could not be performed below 200 K, due to the too high resistance.[8,15] The temperature dependence of the resistance of $LaVO_3$ on DSO(110)[8] is in stark contrast to the behavior of the resistance of $LaVO_3$ films on STO(100) substrates, for which metallic-like behavior was measured by several groups.[4,7,8] DSO, which is a better insulator and is less prone to become oxygen deficient or get reduced,[11,31] preserves an insulating surface during and after the $LaVO_3$ deposition. Temperature-dependent *dc* resistivity measurements of $LaVO_3$ single crystals show the onset of the G-type OO by the kinks in the curve, occurring at 141 K.[1] However, no similar kinks have been observed or reported for resistivity data on thin film $LaVO_3$ samples on various substrates.[4,7–9,21]

A convenient method to study the OO transition in bulk $LaVO_3$ is Raman spectroscopy. The Raman spectra of $LaVO_3$ show the activation of a characteristic band at 719 cm^{-1} (89 meV) below the OO transition.[2,16–18,20] This band is readily observed using excitation resonant to the Mott-Hubbard gap near 2 eV, such as the light of a HeNe laser (1.96 eV).[16,17,19] It originates from an out-of-phase oxygen stretching mode along the *c*-axis and has a B_{1g} symmetry in the orthorhombic *Pbnm* phase and a *Ag* symmetry in the monoclinic OO phase.[2,16–18,32] This Raman mode was observed for $LaVO_3$ crystals for *xx*-polarized light and not for *zz*-polarized light (the relations of the optical axes, x, y, and z, to the orthorhombic axes a, b, c are $x = a + b$, $y = a - b$, and

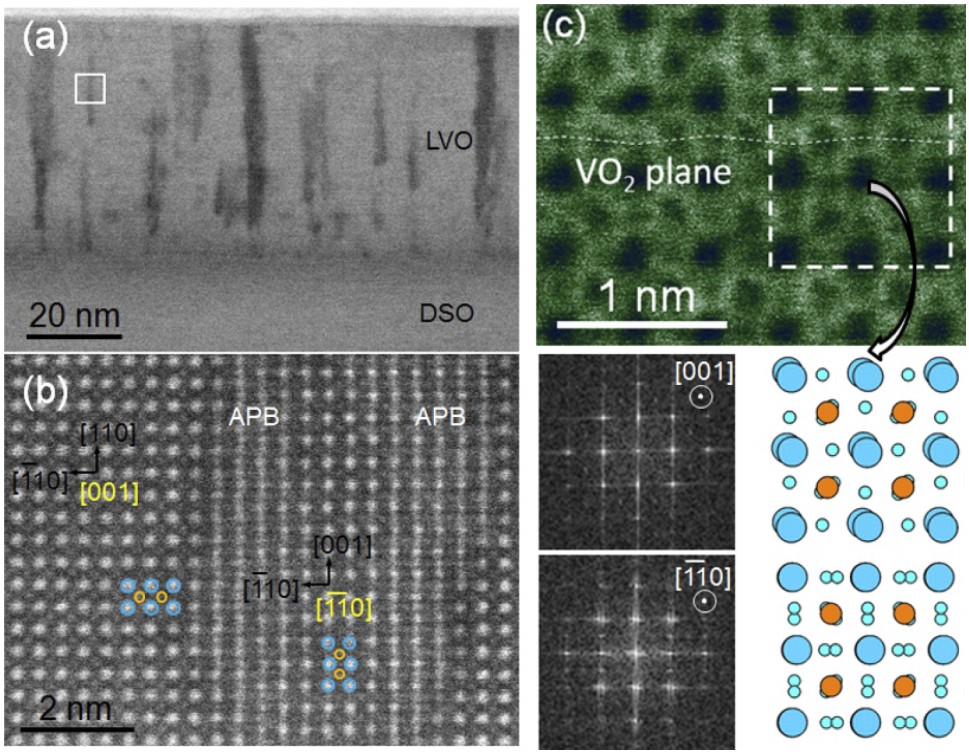

FIG. 3. Cross section HAADF- and ABF-STEM investigations of a 52 nm thick $LaVO_3$ film grown on $DyScO_3(110)$: (a) low magnification overview image with a white box indicating where the high magnification images from (b) were taken; (b) high magnification image of a region where two domains, separated by anti-phase boundaries (APB), are visible: a domain with the in-plane $[001]_o$ c-axis pointing to the viewer, a domain with the out-of-plane $[001]_o$ c-axis pointing to the top surface, and their corresponding fast Fourier transforms (FFT) with structure models at the right; (c) high magnification ABF-STEM image taken in a domain with the $[001]_o$ c-axis pointing to the viewer where the oxygen atomic columns are also imaged and the tilts of the VO_6 octahedra are visible.

$z = c$).[2,16,17,19] We monitored this particular Raman peak in the spectra of a 55 nm thick $LaVO_3$ film grown on DSO(110) substrate. This $LaVO_3$ film was capped with ≈1.5 nm thick amorphous $SrTiO_3$ layer to protect it against oxidation.[33] Figure 4 shows the spectra acquired while heating the sample from 87 K to RT. Three peaks clearly observed at about 182 cm^{-1} (23 meV), 427 cm^{-1} (53 meV), and 717 cm^{-1} (89 meV) at 88 K (as marked by black arrows) can be assigned to the $LaVO_3$ film (Fig. 4(a)). The first two peaks persist in the Raman spectra up to RT: the one at 182 cm^{-1} (23 meV) is related to the rotation of VO_6 octahedra and the one at 427 cm^{-1} (53 meV) corresponds to the Jahn-Teller mode.[16,17] The *Ag* out-of-phase oxygen stretching mode at 717 cm^{-1} (89 meV) disappears at about 160 K (Fig. 4(b)), indicating that OO transition temperature in the $LaVO_3$ film is ≈160 K (Fig. 4(c)). This transition temperature to the G-type OO phase is slightly higher than for bulk crystals. Such a shift is not uncommon in epitaxial strained films and may be due to epitaxy induced structural modifications. It was recently found that in single crystals of $Y_{1-x}La_xVO_3$, G-type OO is present locally above the T_{OO} temperature, but it is short range.[34]

We also measured Raman scattering spectra of $LaVO_3$ films grown on STO(100) substrate down to 87 K (not shown). $SrTiO_3$ is not a good substrate for Raman investigations of thin films samples because it exhibits multiple phonon modes and a strong Raman background that substantially hinder Raman-based thin film experiments.[35] This is in particular true for probing the OO in $LaVO_3$ films since STO has a dominant spectral feature at 716 cm^{-1} (88.7 meV), preventing the unambiguous observation of the 719 cm^{-1} (89 meV) G-type OO-related phonon of $LaVO_3$.

More insight into the OO of the $LaVO_3$ films under compressive strain could be, however, obtained by Raman spectroscopy of (110)/(001)-oriented $LaVO_3$ films grown on LGO(110)/(001) substrates (Fig. 5). LGO crystals allow the observation of the $LaVO_3$ phonons at 270 cm^{-1} (33 meV,

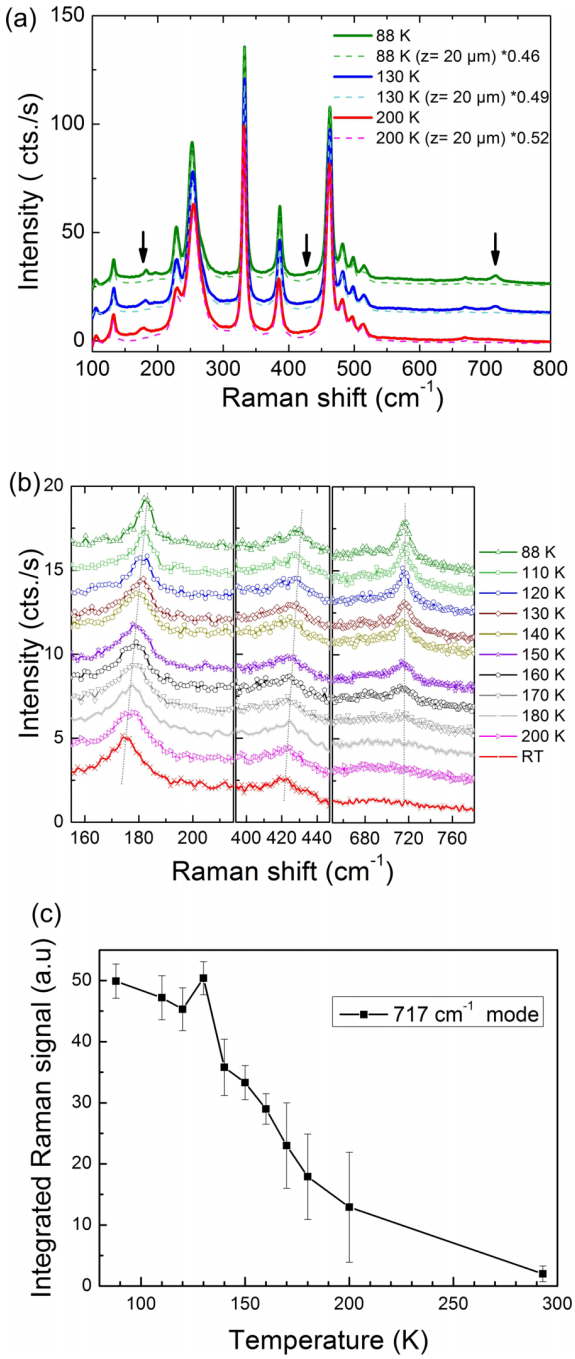

FIG. 4. Temperature-dependent Raman scattering spectroscopy of a 55 nm thick $LaVO_3$ film grown on $DyScO_3$(110), capped with amorphous $SrTiO_3$: (a) Raman spectra at temperatures above and below the OO-transition, focusing at the sample surface (i.e., film/substrate signal, thick lines) and 20 μm below the surface (substrate signal only, thin dashed lines); the black arrows point at Raman peaks corresponding to the $LaVO_3$ film. (b) Detailed temperature dependence of the three observed Raman scattering peaks belonging to the $LaVO_3$ film was obtained by normalizing the two spectra at the same intensity and their subsequent subtraction. (c) Temperature dependence of the integrated intensity for the Raman peak occurring at about 717 cm^{-1}, evidencing the transition toward orbital ordering ($T_{OO} \approx 160$ K) in $LaVO_3$ films grown under tensile strain.

an oxygen bending mode that is active already at RT, see Ref. 17), 348 cm^{-1} (43 meV) and 513 cm^{-1} (63 meV), and at about 700-725 cm^{-1} (86-90 meV) (Fig. 5(a)). Around 700 cm^{-1} (86 meV), a broad peak is visible already at RT which it splits into two peaks at 90 K, one at 701 cm^{-1} (86 meV) and one at 725 cm^{-1} (90 meV). The former was attributed to the phonon density of states[18] and the

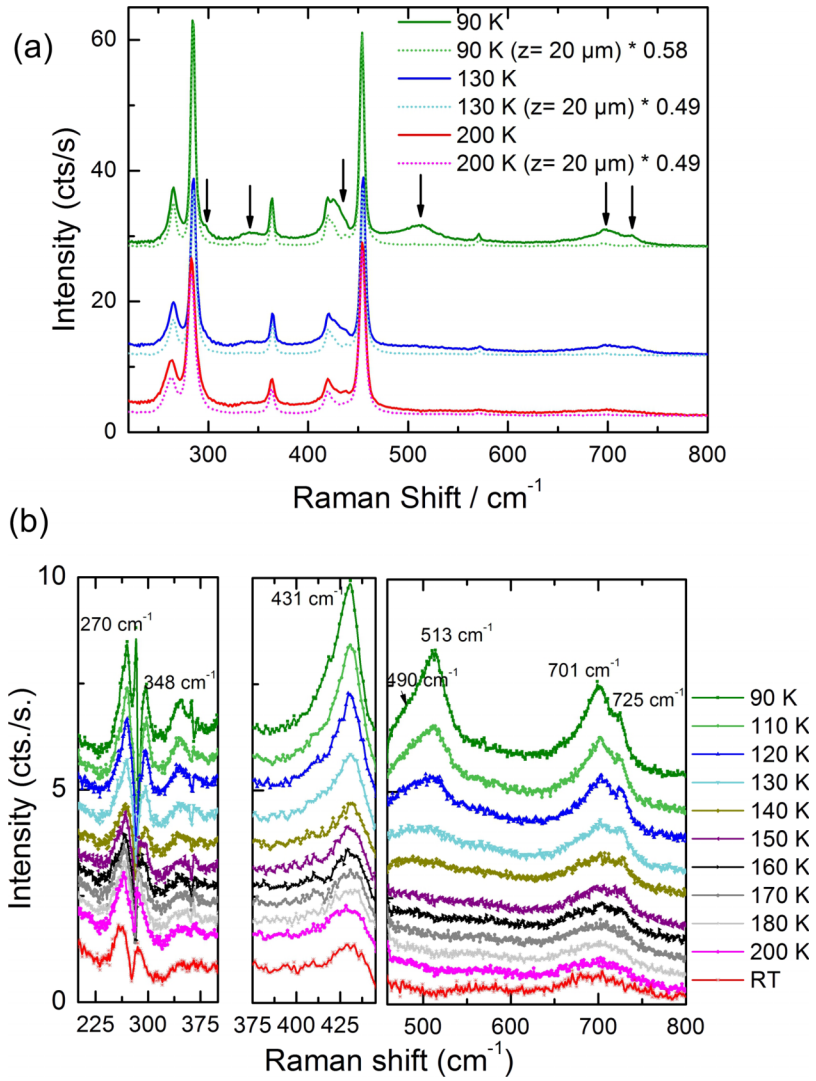

FIG. 5. Temperature-dependent Raman scattering spectroscopy of a 55 nm thick $LaVO_3$ film grown on a twinned $LaGaO_3$(110)/(001) crystal: (a) Raman spectra at temperatures above and below the OO-transition, focusing at the sample surface (i.e., film/substrate signal, thick lines) and 20 μm below the surface (substrate signal only, thin dashed lines); the black arrows point at Raman peaks corresponding to the $LaVO_3$ film. (b) Detailed temperature dependence of the observed Raman scattering peaks belonging to the $LaVO_3$ film was obtained by normalizing the two spectra at the same intensity and their subsequent subtraction. The Raman band at about 270 cm^{-1} was affected by the subtraction procedure, because of the close proximity of a strong Raman mode of the $LaGaO_3$ crystal.

latter has been assigned to the A_g out-of-phase oxygen stretching mode. For LaVO3/LGO(110), the mode is shifted to higher energy as compared to the mode in $LaVO_3$/DSO(110) samples, in which it occurs at 717 cm^{-1} (89 meV) at 88 K. This energy difference indicates that compressive and tensile epitaxial strain influences the structure of $LaVO_3$ epitaxial films.

In addition to the characteristic phonon peak around 720 cm^{-1} (89 meV) clearly evidencing the structural phase transition and the onset of G-type OO in $LaVO_3$, the spectra of the $LaVO_3$/LGO sample (Fig. 5(b)) also show the appearance of two broad Raman bands at 348 cm^{-1} (43 meV) and 513 cm^{-1} (63 meV) below 160 K. These modes, which are also characteristic for the OO phase,[36] have been reported by Miyasaka *et al.*, who showed them to be resonantly enhanced when exciting at the Mott-Hubbard gap energy.[16,17] Even though it is generally agreed that these modes are associated with the OO phase, the precise origin of these modes is currently not clear. Miyasaka *et al.* assigned them to collective electronic excitations (two-orbiton excitations). Sugai and Hirota[37]

argued that this assignment might be incorrect and that, for instance, the 513 cm^{-1} (63 meV) band is more likely due to a Jahn-Teller phonon, in analogy to similar modes in other orthorhombic perovskites.[32] It may be that these modes originate even from multi-phonon processes, as it was debated in the case of similar modes observed in OO phase of $LaMnO_3$.[38]

Summarizing, we fabricated epitaxial films of $LaVO_3$ on various crystals by PLD under reducing Ar/H_2 atmosphere and characterized their domain structure by high resolution scanning transmission electron microscopy. By Raman scattering spectroscopy, for the first time, we evidenced that the transition to orbital ordering occurs in $LaVO_3$ films, both under compressive and tensile strain. This enables the study of further aspects of orbital ordering, such as the influence of compressive *vs*. tensile strain and epitaxy-induced deformations of oxygen octahedra on the orbital-ordering and electronic structure of film samples. Raman scattering spectroscopy in conjunction with future temperature-dependent optical conductivity[19,30] and X-ray spectroscopy[39] measurements corroborated with VO_6 octahedra observations by electron microscopy can provide a comprehensive insight into the structure-electronic property relations of epitaxially modified $LaVO_3$.

I.V. thanks Chencheng Xu, Felix Hensling, Christoph Bäumer, and Dr. Paul Meuffels for kind assistance at PGI-7, Forschungszentrum Jülich. I.V. is also thankful to Professor Markus Grüninger and Professor Thomas Lorenz from II. Physics Institute of University of Cologne and to Dr. Eva Benckiser from MPI-FKF, Stuttgart for helpful discussions.

[1] S. Miyasaka, T. Okuda, and Y. Tokura, Phys. Rev. Lett. **85**, 5388 (2000).
[2] S. Miyasaka, Y. Okimoto, M. Ywama, and Y. Tokura, Phys. Rev. B **68**, 100406(R) (2003).
[3] E. Janod, J. Tranchant, B. Corraze, M. Querré, P. Stoliar, M. Rozenberg, T. Cren, D. Roditchev, V. T. Phuoc, M.-P. Besland, and L. Cario, Adv. Funct. Mater. **25**, 6287 (2015).
[4] Y. Hotta, T. Susaki, and H. Y. Hwang, Phys. Rev. Lett. **99**, 236805 (2007).
[5] Y. Hotta, Y. Mukunoki, T. Susaki, H. Y. Hwang, L. Fitting, and D. A. Muller, Appl. Phys. Lett. **89**, 031918 (2006).
[6] M. L. Scullin, J. Ravichandran, C. Yu, M. Huijben, J. Seidel, A. Majumdar, and R. Ramesh, Acta Mater. **58**, 457 (2010).
[7] H. Rotella, O. Copie, A. Pautraut, P. Boullay, A. David, D. Pellouquin, C. Labbe, C. Frilay, and W. Prellier, J. Phys.: Condens. Matter **27**, 095603 (2015).
[8] C. He, T. D. Sanders, M. T. Gray, F. J. Wong, V. V. Mehta, and Y. Suzuki, Phys. Rev. B **86**, 081401(R) (2012).
[9] F. S. Razavi, S. Jamali Gharetape, D. A. Crandles, G. Christiani, R. K. Kremer, and H.-U. Habermeier, Appl. Phys. Lett. **96**, 042110 (2010).
[10] F. J. Wong, S.-H. Baek, R. V. Chopdekar, V. V. Mehta, H.-W. Jang, C.-B. Eom, and Y. Suzuki, Phys. Rev. B **81**, 161101 (2010).
[11] C. W. Schneider, M. Esposito, I. Marozau, K. Conder, M. Doebeli, Y. Hu, M. Mallepell, A. Wokaun, and T. Lippert, Appl. Phys. Lett. **97**, 192107 (2010).
[12] X. Ke, C. Adamo, D. G. Schlom, M. Bernhagen, R. Uecker, and P. Schiffer, Appl. Phys. Lett. **94**, 152503 (2009).
[13] A. V. Mahajan, D. C. Johnston, D. R. Torgeson, and F. Borsa, Phys. Rev. B **46**, 10966 (1992).
[14] N. H. Hur, S. H. Kim, K. S. Yu, Y. K. Park, and J. C. Park, Solid State Commun. **92**, 541 (1994).
[15] O. Copie, H. Rotella, P. Boullay, M. Morales, A. Pautrat, P.-E. Janolin, I. C. Infante, D. Pravathana, U. Lüders, and W. Prellier, J. Phys.: Condens. Matter **25**, 492201 (2013).
[16] S. Miyasaka, S. Onodo, Y. Okimoto, J. Fujioka, M. Ywama, N. Nagaosa, and Y. Tokura, Phys. Rev. Lett. **94**, 076405 (2005).
[17] S. Miyasaka, J. Fujioka, M. Ywama, Y. Okimoto, and Y. Tokura, Phys. Rev. B **73**, 224436 (2006).
[18] B. Roberge, S. Jandl, A. A. Nugroho, T. T. M. Palstra, L. D. Tung, and G. Balakrishnan, J. Raman Spectrosc. **46**, 1157 (2015).
[19] S. Miyasaka, Y. Okimoto, and Y. Tokura, J. Phys. Soc. Jpn. **71**, 2086 (2002).
[20] J. Fujioka, S. Miyasaka, and Y. Tokura, Phys. Rev. Lett. **97**, 196401 (2006).
[21] I. Chaitanya Lekshami, A. Gayen, and M. S. Hegde, J. Phys. Chem. Solids **66**, 1647 (2005).
[22] H.-T. Zhang, L. R. Dedon, L. W. Martin, and R. Engel-Herbert, Appl. Phys. Lett. **106**, 233102 (2015).
[23] A. Shkabko, C. Xu, P. Meuffels, F. Gunkel, R. Dittmann, A. Weidenkaff, and R. Waser, APL Mater. **1**, 052111 (2013).
[24] M. Hepting, M. Minola, A. Frano, G. Cristiani, G. Logvenov, E. Schierle, M. Wu, M. Bluschke, E. Weschke, H. U. Habermeier, E. Benckiser, M. Le Tacon, and B. Keimer, Phys. Rev. Lett. **113**, 227206 (2014).
[25] P. Bordet, C. Chaillout, M. Marezio, Q. Huang, A. Santoro, S.-W. Cheong, H. Takagi, C. S. Oglesby, and B. Batlogg, J. Solid State Chem. **106**, 253 (1993).
[26] H. Rotella, O. Copie, G. Steciuk, H. Ouerdana, P. Boullay, P. Roussel, M. Morales, A. David, A. Pautraut, B. Mercey, L. Lutterotti, D. Chateigner, and W. Prellier, J. Phys.: Condens. Matter **27**, 175001 (2015).
[27] G. Sclauzero and C. Ederer, Phys. Rev. B **92**, 235112 (2015).
[28] T. Ohnishi, K. Shibuya, T. Yamamoto, and M. Lippmaa, J. Appl. Phys. **103**, 103703 (2008).
[29] H. Rotella, U. Lüders, P.-E. Janolin, V. H. Dao, D. Chateigner, R. Feyerherm, E. Dudzik, and W. Prellier, Phys. Rev. B **85**, 184101 (2012).
[30] J. Reul, A. A. Nugroho, T. T. M. Palstra, and M. Grüninger, Phys. Rev. B **86**, 125128 (2012).
[31] G. Yuan, K. Nishino, M. Lippmaa, and A. Uedono, J. Phys. D: Appl. Phys. **43**, 025301 (2010).

[32] M. N. Iliev, M. V. Abrashev, H.-G. Lee, V. N. Popov, Y. Y. Sun, C. Thomsen, R. L. Meng, and C. W. Chu, Phys. Rev. B **57**, 2872 (1998).
[33] H. Wadati, Y. Hotta, M. Takizawa, A. Fujimori, T. Susaki, and H. Y. Hwang, J. Appl. Phys. **102**, 053707 (2007).
[34] S. Yano, D. Louca, J. C. Neuefeind, J.-Q. Yan, J.-S. Zhou, and J. B. Goodenough, Phys. Rev. B **90**, 214111 (2014).
[35] L. Gasparov, T. Jegorel, L. Loetgering, S. Middey, and J. Chakhalian, J. Raman Spectrosc. **45**, 465 (2014).
[36] S. Ishihara, Phys. Rev. B **69**, 075118 (2004).
[37] S. Sugai and K. Hirota, Phys. Rev. B **73**, 020409(R) (2006).
[38] M. Grüninger, R. Rückamp, M. Windt, P. Reutler, C. Zobel, T. Lorenz, A. Freimuth, and A. Revcolevschi, Nature **418**, 39 (2002).
[39] B. Chen, J. Laverock, D. Newby, Jr., J. F. McNulty, K. E. Smith, P.-A. Glans, J.-H. Guo, R.-M. Qiao, W.-L. Yang, M. R. Lees, L. D. Tung, R. P. Singh, and G. Balakrishnan, J. Phys.: Condens. Matter **27**, 105503 (2015).